Identification of Body Fat Tissues in MRI Data

Dana Ilea[a], Ovidiu Ghiță[b], Kevin Robinson[b], Robert Sadleir[b], Michael Lynch[b], Darren Brennan[c], and Paul F. Whelan[b], *Senior Member, IEEE*

[a]Faculty of Electrical Engineering and Computers,
Transilvania University Brasov, Romania

[b]Vision Systems Group,
School of Electronic Engineering,
Dublin City University, Glasnevin, Dublin, Ireland

[c]Cappagh National Orthopaedic Hospital
Finglas, Dublin, Ireland

***Abstract*-- In recent years non-invasive medical diagnostic techniques have been used widely in medical investigations. Among the various imaging modalities available, Magnetic Resonance Imaging is very attractive as it produces multi-slice images where the contrast between various types of body tissues such as muscle, ligaments and fat is well defined. The aim of this paper is to describe the implementation of an unsupervised image analysis algorithm able to identify the body fat tissues from a sequence of MR images encoded in DICOM format. The developed algorithm consists of three main steps. The first step pre-processes the MR images in order to reduce the level of noise. The second step extracts the image areas representing fat tissues by using an unsupervised clustering algorithm. Finally, image refinements are applied to reclassify the pixels adjacent to the initial fat estimate and to eliminate outliers. The experimental data indicates that the proposed implementation returns accurate results and furthermore is robust to noise and to greyscale in-homogeneity.**

***Index Terms*—MRI, Body fat, Image de-noising, Image segmentation, Clustering, Region growing.**

I. Introduction

The accurate determination of a person's total body fat is an important issue in medical analysis as obesity is a significant contributing factor to a variety of serious health problems. The medical literature identifies a wide range of diseases that are closely related to obesity including hypertension, coronary heart disease, strokes, gout, diabetes, various types of cancer and psychological disorders such as depression and low self-esteem [5].

In the past the evaluation of total body fat has included techniques such as hydro-density, callipers and air displacement (Bod Pod). The accuracy of these techniques is limited and furthermore the results are subject to inter and intra observer variability. More recently, new techniques have been developed and among them the most important are DEXA, NIR and TOBEC (more details about these techniques can be found in [5]). In most cases these techniques are accurate but the equipment is dedicated and expensive and this is a deterring factor for their application in current medical investigations. On the other hand Magnetic Resonance Imaging (MRI), although expensive, is used extensively for many types of medical investigations and as such MRI facilities are available more readily and widely.

Alternative medical techniques have been used to measure the body fat such as Computer Tomography (CT) and MRI. As in the past the quality of MRI images was limited, CT was widely used to measure the total body fat. The results proved to be very encouraging but it should be mentioned that due to the effect of the ionising radiation involved this technique is rendered impractical for serial investigations [8]. With the advancement in medical imaging, current MRI produces high-resolution volumetric image sequences and it becomes an attractive imaging modality to measure body fat.

In our investigation we attempt to extract the areas representing fat tissues in a sequence of MR images. The image segmentation task has to be able to accommodate problems such as greyscale in-homogeneity within the regions representing fat tissues and a relatively low signal to noise ratio. In order to address these issues firstly we pre-process the input data to reduce the noise level. Then, the pre-processed data is roughly segmented using an unsupervised clustering method. Finally, the result is further improved by applying image refinements to eliminate misclassified pixels.

This paper is organised as follows. In this section we have introduced the problem to be investigated. Section 2 details the segmentation algorithm. Section 3 presents some experimental results and Section 4 concludes the paper.

II. IMAGE SEGMENTATION

A visual examination of the images contained in the data sets reveals that the fat tissues tend to have a higher grayscale value than other tissues. But these images also indicate that there is quite a high grayscale variation within the image regions which represent fat tissues and in some situations their grayscale values are lower than those associated with other tissues such as those representing bones, liver or brain. Therefore, accurate segmentation cannot be achieved by applying simple methods based on thresholding.

Thus, in order to cope with these problems we have devised a three-step segmentation algorithm. The first step involves pre-processing the input image in order to reduce the level of noise. As a visual examination indicates that the imaged fat tissues always have their grayscale values higher than 100, we eliminate from the input data the information that has grayscale values below this threshold. Then, we reduce the level of speckle noise by applying a median filter which is followed by the application of a feature–preserving adaptive smoothing operator. The adaptive smoothing operator is applied to eliminate the Gaussian distributed noise while preserving the high-gradient image information (i.e. image edges). The aim of this pre-processing scheme is to achieve a smooth de-noised image. The next section will briefly introduce the adaptive smoothing operator used in this implementation.

A. Adaptive smoothing operator

The aim of this operation is to remove the additive image noise while preserving the image edge information. To this end, we implemented the smoothing algorithm described in [2]. This smoothing algorithm tries to adapt pixel intensities to the local attributes present in the image by evaluating two discontinuity measures (i.e. local and contextual) that should be preserved during the smoothing operation.

The local discontinuity is measured using four detectors that approximates the image gradients in four directions:

$$\begin{aligned} E_{Hxy} &= \left| I_{x+1,y} - I_{x-1,y} \right|, \\ E_{Vxy} &= \left| I_{x,y+1} - I_{x,y-1} \right|, \\ E_{Cxy} &= \left| I_{x+1,y+1} - I_{x-1,y-1} \right|, \\ E_{Dxy} &= \left| I_{x+1,y-1} - I_{x-1,y+1} \right| \end{aligned} \tag{1}$$

where $I_{x,y}$ is the pixel intensity at *(x,y)*. These four detectors respond strongly to local edges and a local discontinuity measure can be defined as follows:

$$E_{x,y} = \frac{E_{Hxy} + E_{Vxy} + E_{Cx,y} + E_{Dx,y}}{4} \tag{2}$$

As the local discontinuity evaluates the local gradients it is sensitive to image noise. Unfortunately, the MR images reveal a high level of noise and as a result the local discontinuity is not efficient in distinguishing the true local discontinuities from noise. Thus, the local discontinuity has to be augmented with a contextual discontinuity, which evaluates the attributes of the neighboring pixels.

In this implementation the contextual discontinuities are measured by the local variance that is measured in a predefined neighborhood (see Eq. 3).

$$\sigma^2_{xy}(R) = \frac{\sum_{(i,j \in N_{xy}(R))} (I_{i,j} - \mu_R)^2}{N_{xy}(R)} \tag{3}$$

where σ^2_{xy} is the measured variance, μ_R is the mean intensity value computed in the square neighborhood R.

The adopted smoothing strategy uses both local and contextual discontinuities and for each pixel its intensity value is iteratively updated with the nonlinear transformation illustrated in Eq. (4).

$$I^{t+1}_{xy} = I^t_{xy} + \eta_{xy} \frac{\sum_{(i,j)\in N_{xy}(1)\setminus\{x,y\}} \eta_{ij}\gamma^t_{ij}(I^t_{i,j} - I^t_{x,y})}{\sum_{(i,j)\in N_{xy}(1)\setminus\{x,y\}} \eta_{ij}\gamma^t_{ij}} \tag{4}$$

where,

$$\eta_{ij} = \exp(-\alpha\Phi(\sigma^2_{xy}(R), \theta_\sigma)) \tag{5}$$

$$\gamma^t_{ij} = \exp(-E^t_{ij} / S) \tag{6}$$

$$\Phi(\sigma^2_{xy}(R), \theta_\sigma) = \begin{cases} 0 & \sigma^2_{xy}(R) < \theta_\sigma \\ \sigma^2_{xy}(R) & \sigma^2_{xy}(R) \geq \theta_\sigma \end{cases} \tag{7}$$

In Eqs. 4 to 6 the parameter *t* defines the iteration and the transformation illustrated in Eq. 4 updates the intensity values of each pixel using two weighting parameters (η and γ) which measure non-linearly the contextual and local discontinuities. The variables S and α are important as they determine to what extent the local and contextual discontinuities should be preserved during the smoothing operation.

In our implementation we set these parameters to the following values S = 10, α=10, θ_σ =0.2, window size R =2, and the algorithm is run for 2 iterations.

Fig 1 illustrates the performance of the adaptive smoothing operation. Note that the smoothing operation did not affect the edge localization.

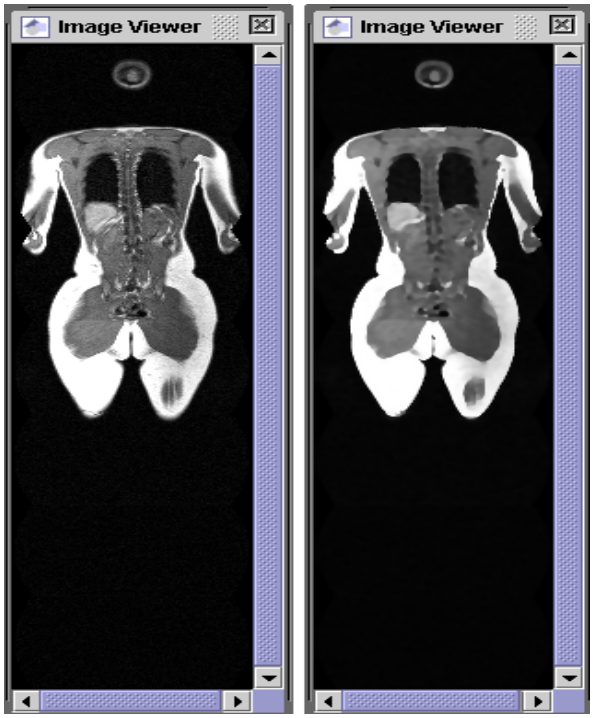

(a) (b)

Fig. 1. Adaptive smoothing operation. (a) Input image.

(b) Filtered image.

B. Clustering and Image Refinements

The second step involves the application of unsupervised clustering [3] on the image obtained from the first step. For this implementation we have used an agglomerative clustering technique [1] where the parameters for inter-cluster variation are set to 0.8 for lower threshold and 1.2 for higher threshold. The number of resulting clusters is dependent on the complexity of the input image. To extract the data clusters associated with body fat tissues we applied a threshold operation where the threshold value is set to 120. As some input images (especially those from the beginning and the end of the sequence) show areas where the noise signal is amplified (see Fig. 2) we have to eliminate the small areas defined by bright pixels. It should be noted that some of these pixels have been removed by the pre-processing scheme (see for example Fig. 3b).

Experimentation indicated that the image bright areas derived from fat tissues will consist of more than 20 pixels. Thus we have eliminated regions with fewer than 20 pixels by applying a label by area operation. The algorithm evaluates each labeled image starting with the smallest label and those that have less than 20 pixels are eliminated.

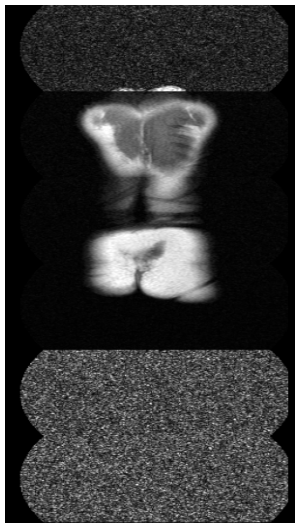

Fig. 2. Input image showing large image areas defined by noise.

The image resulting from the second step is subjected to the application of image refinements as some other tissues (e.g. brain and liver) are misclassified as body fat. For this purpose the following strategy has been employed. Each image pixel (resulting from step 2) that has been classified as fat (marked in white) is evaluated in its 3x3 neighborhood and the pixels that have a grayscale value larger than 150 are counted. If inside this 3x3 neighborhood more than half of the total number of pixels have values larger than 150 then the pixel is deemed to have been correctly classified. Otherwise the pixel is considered to have been misclassified and it is reclassified as background. This strategy is the 2D version of that described in [4]. The aim of this algorithmic scheme is to eliminate significant misclassified areas.

The next step is applied to improve the segmentation by reclassifying the pixels adjacent to segmented areas. For this strategy we employed a region growing technique which is based on the morphological dilation operation [9]. This algorithm has two inputs, namely the original image and the segmentation result obtained after the previous step is completed. The segmented image is in binary form where the fat tissues are marked in white while the rest of the tissues are background. The algorithm dilates the binary image with a 3x3 square structuring element and the dilated pixels are reclassified as fat tissue only if their grayscale values are above a threshold value that has been experimentally set to 130. This strategy is iteratively applied until no pixels are reclassified. The aim of this operation was to fill the gaps in the segmented structure and close the boundary discontinuities.

III. Experiments And Results

The algorithm described in Section 2 has been implemented using the NeatVision 2.0 Java graphical development environment [6]. The segmented data is a binary volume where the voxels defined by fat tissues are marked in white while the background is marked with black.

The calculation of the total body fat (TBF) involves the formula shown in Eq. 8.

$$TBF = N_{FatVoxels} * Voxel\_Dim * Fat\_Density \quad (8)$$

where $N_{FatVoxels}$ is the total number of fat voxels contained in the dataset, *Voxel_Dim* is the voxel dimension (in cm^3), and *Fat_Density* is the density of the fat tissue. The voxel dimension can be extracted from the DICOM header and the datasets used in our study have a dimension of $2.02 \times 2.02 \times 8$ [mm^3]. The medical literature indicates that the fat tissue density is constant [7] and it has a value of 0.918 [g/cm^3]. The number of fat voxels is determined by counting the white voxels contained in the segmented data. We normalized these values in order to yield the total body fat in kilograms.

A database of 19 datasets (9 males and 10 females) was used to assess the validity of the proposed segmentation algorithm. The body mass index (BMI) values of these datasets range from 19 to 32. The BMI is a measure commonly used to assess people's level of fitness in terms of anthropometric measurements. BMI values are classified into 4 categories which are listed in Table I.

TABLE I.
BMI CATEGORIES.

BMI	Category
<18.5	Underweight
18.5-24.9	Normal weight
25-29.9	Overweight
>30	Obese

A visual examination of the datasets used in this study shows a large variation in the grayscale values between similar tissues within the same dataset and from dataset to dataset. A significant level of noise has also been noticed in image areas with a low contrast. As a result we devised a three-component segmentation algorithm to identify the fat tissues as described in the Section II. Figures 3 to 5 depict the segmentation results that were achieved after the algorithm was applied to three representative data sets.

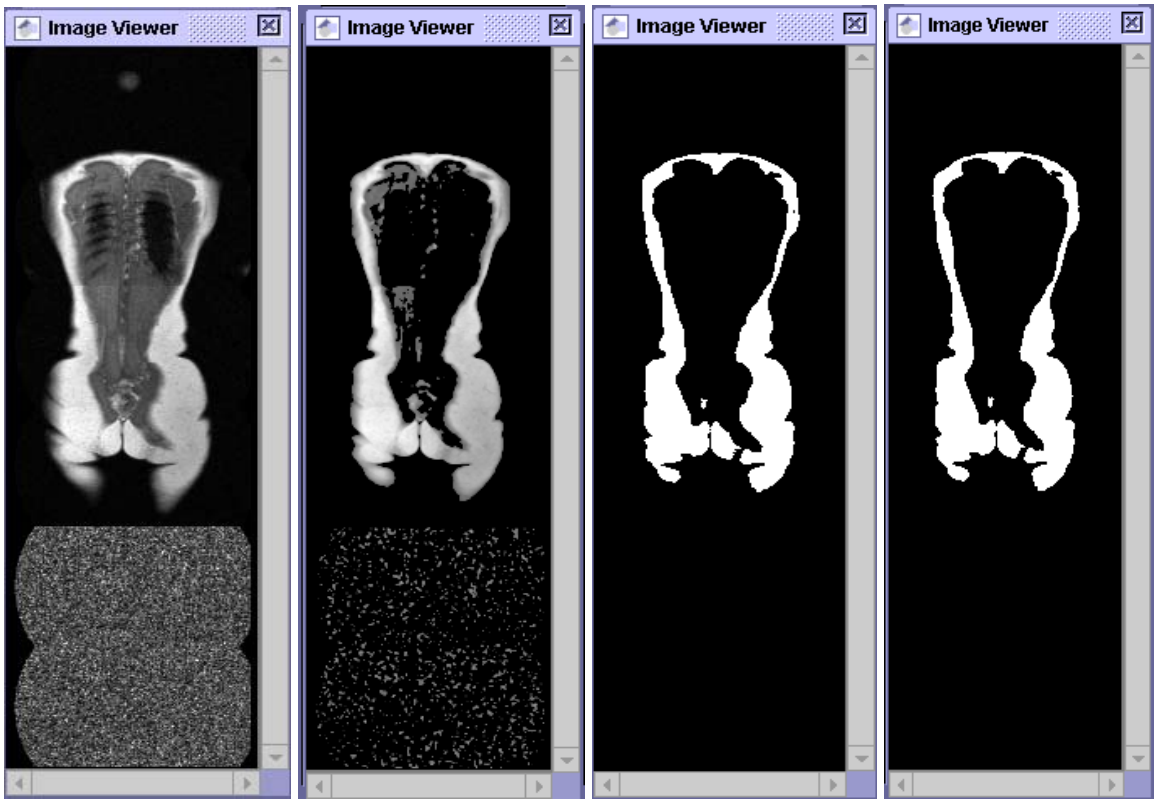

(a) (b) (c) (d)

Fig. 3. Experimental data –dataset 1 (slice 4). (a) Input image. (b) Pre-processed image. (c) Image resulting after clustering (d) Image resulting after image refinements is applied.

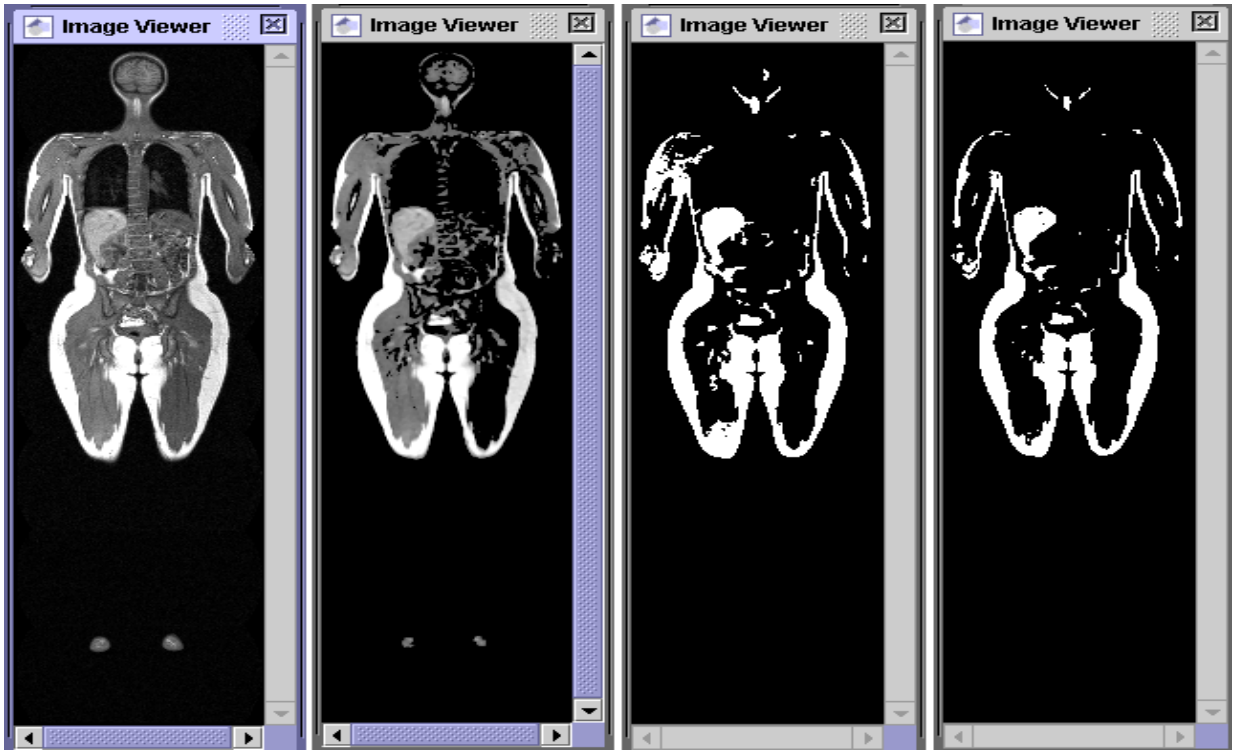

(a) (b) (c) (d)

Fig. 4. Experimental data –dataset 2 (slice 26). (a) Input image. (b) Pre-processed image. (c) Image resulting after clustering. (d) Image resulting after image refinements is applied.

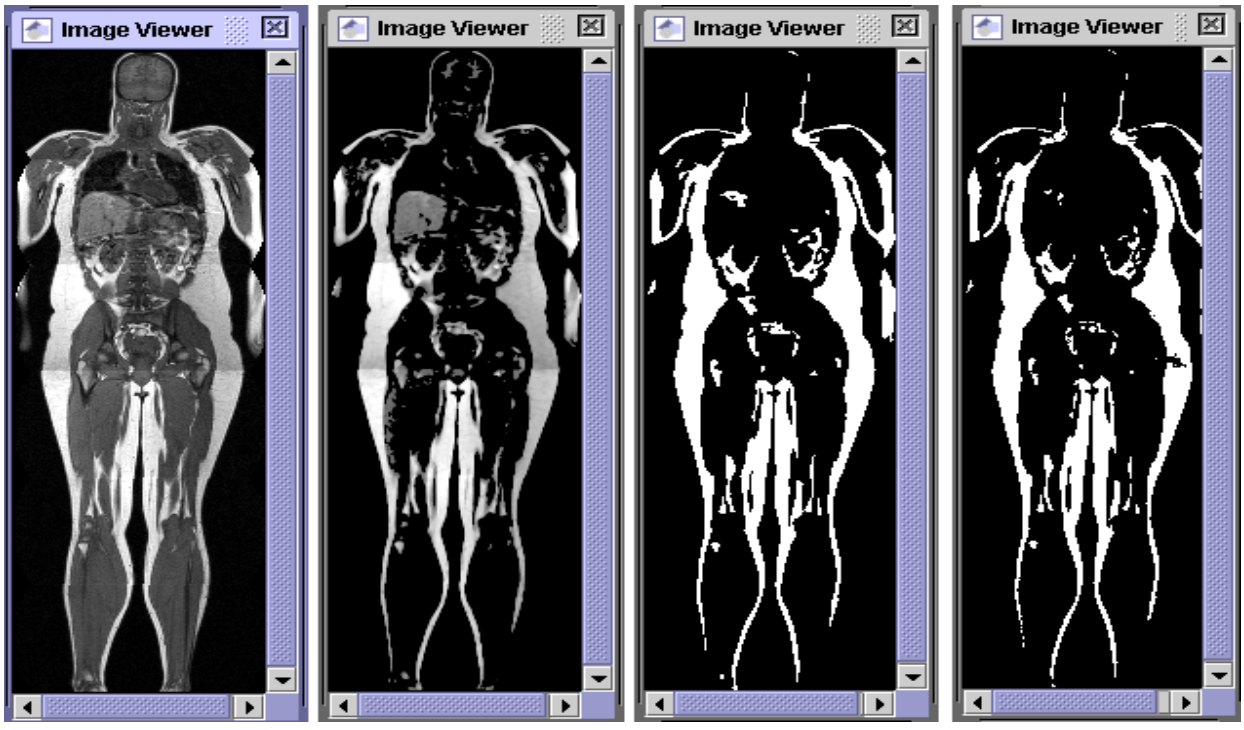

(a) (b) (c) (d)

Fig. 5. Experimental data –dataset 3 (slice 17). (a) Input image. (b) Pre-processed image. (c) Image resulting after clustering. (d) Image resulting after image refinements is applied.

The segmentation results illustrated above indicate the performance of the devised algorithm. The segmentation results for datasets 1 and 3 demonstrate precise fat tissue segmentation. The results obtained for dataset 2 indicate small errors where a part of the liver has been classified as fat tissue. These errors are due to the fact that these tissues have a higher grayscale value than that of most fat tissues in the dataset.

The overall performance of this algorithm has been evaluated on 19 datasets and the results obtained are very encouraging. The algorithm proved to be robust to a high level of image noise and the threshold parameters required by the clustering algorithm and the threshold operations did not need to be readjusted.

As illustrated in these results we have demonstrated that the process of segmenting the body fat is not a trivial one. However we have shown that identification of body fat tissues in MR data is an achievable goal and currently we intend to test the segmentation algorithm on more datasets and have its performance evaluated by a medical practitioner.

IV. Conclusions

This paper described the development of a robust segmentation technique for detection of the body fat tissues in a sequence of MR multi-slice images. The devised algorithm consists of three main components.

The first component performs image de-noising, the second clusters the image data while the third improves the initial segmentation result by applying image refinements.

The developed algorithm proved to be robust in the presence of severe grayscale variation within the image regions representing fat tissue and against the noise introduced in the MR imaging process.

Acknowledgement

We would like to express our gratitude to Cappagh National Orthopaedic Hospital, Dublin, Ireland, for supplying the data sets used in this investigation. This work was carried out during the time Dana Ilea has been an intern student in the Vision System Group, Dublin City University.

References

[1] R. Duda and P.E. Hart, *Pattern classification and scene analysis*, John Wiley & Sons, New York, 1973.

[2] K. Chen, "A feature preserving adaptive smoothing method for early vision", National Laboratory of Machine Perception, Peking University, China, Technical report, 1999.

[3] O. Ghita, P.F. Whelan, and R. Kennedy, "A practical approach for analysing SPI images", *Systemics, Cybernetics and Informatics (SCI 2003)*, Florida, USA, 2003.

[4] K.Y. Kang, K. Engelke, and W.A. Kalender, "A new accurate and precise 3-D segmentation method for skeletal structures in volumetric CT data", *IEEE Transactions on Medical Imaging*, 22(5), pp. 586-598, 2003.

[5] Comparing methods for measuring body fat: http://new-fitness.com/body_fat_analyzing.html

[6] P.F. Whelan, D. Molloy, *Machine Vision Algorithms in Java: Techniques and Implementation*, Springer (London), 2000. NeatVision 2.0 webpage: http://www.neatvision.com.

[7] R.H. Nord, R.K. Payne, "Body composition by dual-energy X-ray absorptiometry - a review of the technology", *Asia Pacific Journal of Clinical Nutrition*, 4(1), pp. 173-175, 1995.

[8] L. Sjostrom, "A computer tomography-based multi-compartment body composition technique and anthropometric predictions of lean body mass, total and subcutaneous adipose tissue", *International Journal of Obesity*, 15, pp.19-30, 1991.

[9] M. Sonka, V. Hlavac, and R. Boyle, *Image Processing, Analysis and Machine Vision*, 2nd edition, Brooks/Cole Publishing Company, 1999.